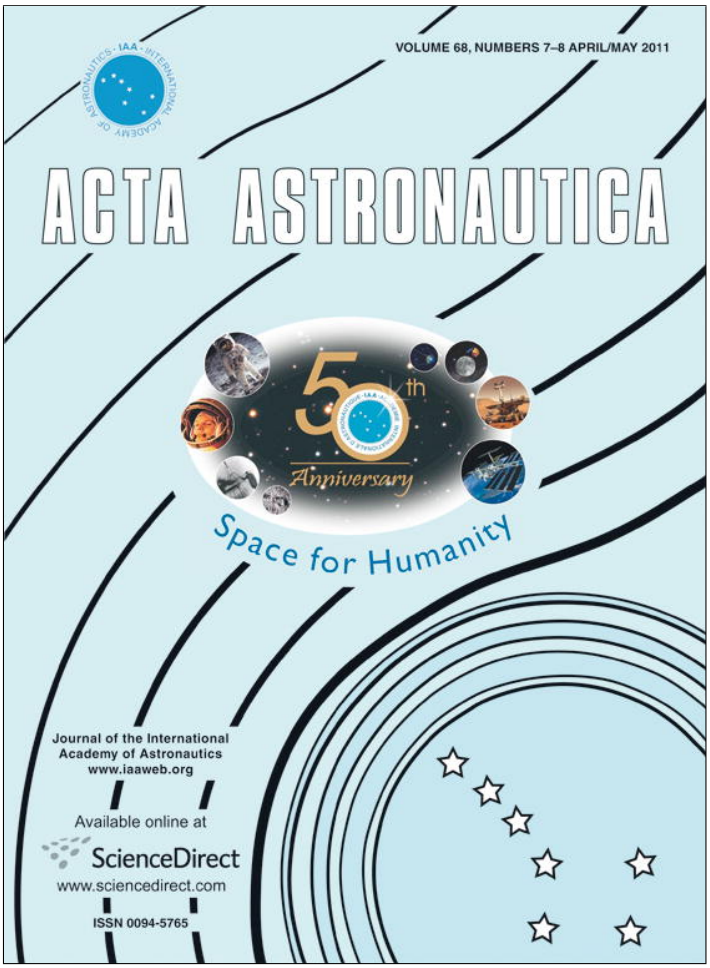

Acta Astronautica 68 (2011) 667–680

Contents lists available at ScienceDirect

Acta Astronautica

journal homepage: www.elsevier.com/locate/actaastro

A Lunar Laser Ranging Retroreflector Array for the 21st Century ☆

Douglas Currie [a,b,c,*], Simone Dell'Agnello [c], Giovanni Delle Monache [c]

[a] Department of Physics, University of Maryland, College Park, College Park MD 20742, USA
[b] NASA Lunar Science Institute, NASA Ames Research Center, Moffett Field, CA, USA
[c] Istituto Nazionale di Fisica Nucleare Laboratori, Nazionali di Frascati, CP 13, Frascati, Italy

ARTICLE INFO

Article history:
Received 7 January 2010
Received in revised form
27 August 2010
Accepted 1 September 2010

Keywords:
Lunar Laser Ranging
Retroreflector
Cube Corner Reflector
NASA Lunar Science Institute
Optical technology
ILN
LLRRA-21
Thermal modeling

ABSTRACT

Over the past 40 years, the Lunar Laser Ranging Program (LLRP) to the Apollo Cube Corner (CCR) Retroreflector Arrays (ALLRRA) [1] has supplied almost all of the significant tests of General Relativity. The LLRP has evaluated the PPN parameters, addressed the possible changes in the gravitational constant and the properties of the self-energy of the gravitational field. In addition, the LLRP has provided significant information on the composition and origin of the moon. This is the only Apollo experiment that is still in operation. Initially the ALLRRAs contributed a negligible fraction of the ranging error budget. Over the decades, the ranging capabilities of the ground stations have improved by more than two orders of magnitude. Now, because of the lunar librations, the existing Apollo retroreflector arrays contribute a significant fraction of the limiting errors in the range measurements.

The University of Maryland, as the Principal Investigator for the original Apollo arrays, is now proposing a new approach to the Lunar Laser Array technology [2]. The investigation of this new technology, with Professor Currie as Principal Investigator, is currently being supported by two NASA programs and by the INFN-LNF in Frascati, Italy. Thus after the proposed installation during the next lunar landing, the new arrays will support ranging observations that are a factor 100 more accurate than the current ALLRRAs.

The new fundamental cosmological physics and the lunar physics [3] that this new Lunar Laser Ranging Retroreflector Array for the 21st Century (LLRRA-21) can provide will be described. In the design of the new array, there are three major challenges: (1) validate the ability to fabricate a CCR of the required specifications, which is significantly beyond the properties of current CCRs, (2) address the thermal and optical effects of the absorption of solar radiation within the CCR, reduce the transfer of heat from the CCR housing and (3) validate an accurate emplacement technique to install the CCR package on the lunar surface. The latter requires a long-term stable relation between the optical center of the array and the deep regolith, that is, below the thermally driven expansion and contraction of the regolith during the lunar day/night cycle.

1. Teams of collaborators

The current degree of success of this project is the result of the support of many individuals and organizations; in particular, a team assembled for the NASA LSSO program and a team assembled as a part of the LUNAR program, centered at the University of Colorado and supported by NLSI.

☆ This paper was presented during the 60th IAC in Daejeon.

* Corresponding author at: Department of Physics, University of Maryland, College Park, College Park, MD 20742, USA
E-mail addresses: currie@umd.edu (D. Currie), Simone.DellAgnello@lnf.infn.it (S. Dell'Agnello), giovanni.dellemonache@lnf.infn.it (G. Delle Monache).

0094-5765/$ - see front matter © 2010 Published by Elsevier Ltd.
doi:10.1016/j.actaastro.2010.09.001

2. Background and overview

The design approach, the computer simulations using Thermal Desktop, Code V and locally developed IDL software, and the results of the thermal vacuum testing conducted at the INFN/LNF's SCF facility at Frascati, Italy for the new array will also be presented. The new lunar CCR housing has been built at INFN/LNF. The innovations in the LLRRA-21 with respect to the Apollo Arrays and the current satellite retroreflector packages will be described. The new requirements for ground stations will be briefly addressed. This new concept for the LLRRA-21 is being considered for the NASA Manned Lunar Landings, for the NASA Anchor Nodes for the International Lunar Network (ILN), for several robotic lander missions and for the proposed Italian Space Agency's MAGIA [4] lunar orbiter mission. See Section 16 for more information on some of the candidate missions for the LLRRA-21.

The University of Maryland led the team that provided NASA with Lunar Laser Ranging Retroreflector Arrays for the Apollo Missions. These were carried to the moon during Apollo 11, Apollo 14 and Apollo 15. After four decades, these arrays are still in operation and are the only experiment on the moon still producing scientific data. In the past 40 years, laser ranging to these arrays has provided most of the definitive tests of the many parameters describing General Relativity.

In addition, the analysis of the Lunar Laser Ranging (LLR) data, in collaboration with some data from other modalities, has greatly enhanced our understanding of the interior structure of the moon [5–8].

However, over the past four decades, the ground station technology has improved by a factor of more than 100, such that the Apollo lunar arrays now contribute a significant portion of the ranging errors. This is due to the lunar librations which are responsible for the "tipping" of the Apollo arrays so that one corner of the array is more distant than the opposite corner by several centimeters. Thus even if a very short laser pulse were sent to the moon, the return pulse would be spread out in time, so one could obtain a range estimate with an accuracy of no better than a few centimeters (for a single shot).

Currently, the University of Maryland leads a program to develop, design and validate LLRRAs that are composed of 100 mm solid CCRs. These new arrays (LLRRA-21) should be capable of supporting ranging accuracies that are a factor of more than 100 better than the Apollo arrays, that is; an accuracy of 10–100 μm, depending upon the mission and mode of emplacement. This may be considered in terms of a Phase I program that addresses deployment on the surface of the regolith that will support single photoelectron ranging accuracies of better than 1 mm. A Phase II program would involve anchoring the CCR to the regolith at a depth of about one meter so that thermal effects in the regolith would not affect the ranging. The Phase II emplacement would support ranging accuracy approaching 10 μm, but it will be many years before the ground stations can take advantage of this accuracy.

This program currently addresses the primary component (i.e., the CCR and the housing) regarding the use of next generation retroreflectors. The details of the mounting and the emplacement procedures will depend upon the mission. For a manned mission (our initial objective), we have considered an array of five CCRs, separated by ten or more meters. These would be anchored to the sub-surface regolith (i.e., at a depth of ~one meter) to escape the diurnal vertical motion of the surface due to solar heating. We also consider robotic missions (ILN, Lunette and X-Google) where, depending upon the available mass and mobility of a possible rover, the configuration may consist of a single or multiple CCRs and/or with surface or anchored emplacements.

This effort is a collaboration of the University of Maryland with the Frascati branch (LNF) of the Institute for Nuclear Physics (INFN) of Italy. This joint effort is addressing the design, analysis, thermal and optical simulation, fabrication and thermal vacuum testing of a concept for the lunar array.

3. Science objectives of the LLRRA-21 program

The science objectives of the overall Lunar Laser Ranging Program (LLRP) address a variety of goals which primarily falls into three categories:

3.1. General Relativity

Almost all of the most accurate tests of General Relativity are currently derived from LLR to the Apollo arrays [9–11]. Over the long term, we expect to improve the current accuracy of these tests by factors as large as 100. This includes many of the PPN parameters as well as G-dot/G ant the violation of the $1/r^2$ law. This will address many tests concerning the validity of General Relativity at a significantly new level of accuracy. This is especially important as we confront two of the major issues in fundamental physics, astrophysics and cosmology: that is, (1) the conflict between the current formulations of General Relativity and Quantum Mechanics and (2) the role and reason for the acceleration of distant galaxies (i.e., Dark Energy).

3.1.1. Equivalence Principle

In general, the Equivalence Principle is fundamental to the Einstein formulation of General Relativity. The Weak Equivalence Principle addresses the interaction between different types on "normal" matter and gravitation. Thus is addresses different types of fundamental particles as well as strong and weak nuclear binding energies. LLR addresses the relative roles of the Einstein formulation and a variety of other proposed theories. Currently LLR demonstrates that the difference in acceleration of the earth and the moon due to the sun is less than 10^{-13} [X1].

3.1.2. Variation of fundamental constants

Our current presumption is that the fundamental constants such at the gravitational constant G do not change over time or over space. The analysis of the 40 years of LLR data indicates that the temporal change in G, i.e., G-dot/G is significantly less than 10^{-12}/yr. Since this much less than the expansion of the external universe, it indicates that the solar system does not participate in this

expansion and thus the expansion is not a fundamental physical phenomenon. Again, the new retroreflectors with a ranging accuracy of less than a millimeter will push this limit another factor of ten.

3.1.3. Explanation of Dark Energy

In the case of Dark Energy, or the anomalous acceleration of very distant galaxies, a theory of additional dimensions of the universe has been proposed in the Dvali–Gabadadze–Porrati model [12] This is one of the theories that would explain the acceleration of the distant galaxies and it predicts and effect that can be tested with lunar ranging. This would require sub-millimeter accuracy in the range would be available with the proposed retroreflectors.

3.2. Lunar science

Much of our knowledge of the interior of the moon is the product of Lunar Laser Ranging [7–10], often in collaboration with other modalities of observation (i.e., seismology and heat flow experiments on the Apollo missions). These physical attributes of the lunar interior include the Love numbers, the existence of a liquid core, the Q of the moon, the physical and free librations of the moon and other aspects of lunar science. Much of this analysis of the laser ranging data to the Apollo retroreflector packages has been carried out by Jim Williams and his group at the Jet Propulsion Laboratory. Some of the areas that will be addressed with the next generation LLRRA-21 are:

Elastic tides of the moon The elastic tidal displacements are characterized by the lunar 2nd-degree Love numbers h_2 and l_2. Tidal distortion of the 2nd-degree gravity potential and moment of inertia depends on the Love number k_2. The Love numbers depend on the elastic properties of the interior including the deeper zones where information is weakest. LLR detects tidal displacements, but determination of k_2 is potentially more accurate but more sensitive to the interior model.

Tidal dissipation The tidal dissipation $\boldsymbol{Q}$ is a bulk property that depends on the radial distribution of the material $\boldsymbol{Q}$s. LLR detects four dissipation terms and infers a weak dependence of tidal $\boldsymbol{Q}$ on frequency. The tidal $\boldsymbol{Q}$s are surprisingly low, but LLR does not distinguish the location of the low-$\boldsymbol{Q}$ material. Low-$\boldsymbol{Q}$ material, suspected of being a partial melt, was found for the zone just above the core, i.e. the interface between the mantle and the liquid core.

Dissipation at liquid-core/solid–mantle interface A fluid core does not share the rotation axis of the solid mantle. While the lunar equator precesses, a fluid core can only weakly mimic this motion. The resulting velocity difference at the core–mantle boundary causes a torque and dissipates energy. Several dissipation terms are considered in the LLR analysis in order to separate core and tidal dissipation. Applying Yoder's turbulent boundary layer theory yields upper limits for the fluid core radius.

Core oblateness During the lunar librations, the fluid core exerts torques on the mantle from fluid motion at an oblate core–mantle boundary (CMB). LLR detects these oblateness effects and has a determination of the fluid moment difference $\boldsymbol{C_f – A_f}$. LLR cannot presently determine the CMB flattening or the fluid core moment.

Lunar moment of inertia Tracking data on orbiting spacecraft gives the second-degree gravity harmonics $\boldsymbol{J_2}$ and $\boldsymbol{C_{22}}$. From LLR one obtains the moment of inertia combinations $\boldsymbol{(C-A)/B}$ and $\boldsymbol{(B-A)/C}$. Combining the two sets gives $\boldsymbol{C/MR^2}$, the polar moment normalized with the mass $\boldsymbol{M}$ and radius $\boldsymbol{R}$. LLR is primarily sensitive to the moment of the solid Moon, without fluid core.

Fluid core moment of inertia The detection of the moment of inertia of the fluid core, using the sidereal terms and the fact that the fluid core responds differently than the solid mantle. Presuming that the core is Fe or FeS (from an analysis of the melting points) the radius is about 390 km. However this can be greatly improved with the incorporation of millimeter ranging.

Search for an inner core A solid inner core might exist inside the fluid core. Gravitational interactions between an inner core and the mantle could reveal its presence. The properties of this inner core are dominated by the different roles of Fe and FeS compounds. At present, this is below the level of detection, but the improved accuracy may yield definitive information, which would also address the possible composition of the inner core region.

Evolution and heating Both tidal and core–mantle dissipation would have significantly heated the Moon when it was closer to the Earth. Early dynamical heating could have approached radiogenic heating helping to promote convection and a dynamo. Evolution studies are aided by a good determination of energy dissipation in the Moon, both tidal Q vs. frequency and CMB.

Free librations The three observed lunar free libration modes are subject to damping so their amplitudes imply active or geologically recent stimulation. If the mode similar to Chandler wobble is stimulated by eddies at the CMB then such activity might be revealed as irregularities in the path of polar wobble.

Selenodetic site positions The Moon-centered locations of the four well-ranged retroreflectors are known with sub-meter accuracy—the most accurately known positions on the Moon. These positions are available as control points for current and future cartographic networks.

Solid inner core The currently undetected effects involve the fluid core free precession and the (expected but undetected) inner core. An inner core would introduce a number of subtle modifications to the lunar rotation, orientation and tides that can be used to learn about its properties.

Elastic tides Elastic tidal displacements are characterized by the lunar 2nd-degree Love numbers h_2 and l_2. Tidal distortion of the 2nd-degree gravity potential and moment of inertia depends on the Love number k_2. Love numbers depend on the elastic properties of the interior including the deeper zones where information is weakest. LLR detects tidal displacements, but determination of k_2 is potentially more accurate but more sensitive to the interior model.

4. Technical challenges of the LLRRA-21

The primary technical objectives of the design of the LLRRA-21 that follow from the scientific objectives are to (1) provide sub-millimeter accuracy of ranging data, (2)

provide adequate laser return to earth-based ground stations and (3) to be stable over the long term – decades – with respect to the deep local regolith.

The major technical/engineering challenges that follow from the scientific objectives are then:

(A) The fabrication of large cube corner reflectors (CCRs) to the required tolerances (the angular tolerances on the back surfaces are ~2.5 times more restrictive than the current state of the art),
(B) The large size of the required material is a challenge w.r.t. the homogeneity of fused silica material,
(C) The thermal control required to reduce the thermal gradients within the CCR to an acceptable level. These thermal gradients produce gradients in the index of refraction that in turn cause the spreading of the return beam and resultant low signal returns,
(D) The goal of the lunar surface emplacement, that is, a long-term stability of 10 μm w.r.t. deep regolith, below the daily thermal expansion motion which can be as large as ~400 μm. For this, we intend to anchor the CCR to regolith at a depth of ~1 m where there is a negligible change in temperature. The CCR will then be supported by a rod of INVAR or silicon carbide with additional temperature compensation performed in the housing.

5. Fabrication challenges

The fabrication of a CCR that would support the LLRRA-21 concept has not been achieved in the past. This requires a CCR that is much larger than any previous CCRs (a factor of 18 in mass compared to the largest of the CCRs fabricated for Apollo arrays and/or satellite systems). This affects the availability of material with the required homogeneity, the fabrication and polishing procedures and the measurement methods. In addition, our tolerances on the back surface angles (i.e., 0.2 arcsec) are more restrictive by a factor of 2.5 than the previous state-of-the-art for laser ranging CCR fabrication. To address this, we have commissioned the fabrication of a 100 mm CCR of the required tolerances and also meet the full documentation required for space flight. This has been accomplished by ITE, Inc. of Beltsville, MD. Two of the angles are a factor of two better (i.e., less than 0.1 arcsec) than our specifications, leading to excellent performance. The material selection is primarily driven by three requirements: (1) it must have an extremely uniform index of refraction (i.e., very good homogeneity) in all three directions, (2) it must be resistant to darkening by cosmic radiation and (3) it must have a very low absorption of solar radiation.

To satisfy these requirements, this demonstration CCR has been fabricated of SupraSil 1 as were the Apollo CCRs. For the next generation of CCRs for LLRRA-21, concerning (1) for the flight CCRs, we plan to use SupraSil 311 which has even better homogeneity, i.e., $\delta n < 10^{-6}$ [13]. Concerning (2) the radiation resistance, the SupraSil 311 specification by Hereaus [13] indicates that there is no visible degradation of the visible transmittance after exposure to Co^{60} □—radiation at a level of 0.063 Mrad/h for 98 h. Concerning (3) the low absorption of solar radiation that produces thermal gradients that in turn distorts the retroreflected beam, the measured transmission of SupraSil 311 [13]. This is then combined with detailed ray traces of the light paths through the CCR that indicates that 3.5% of the solar radiation is absorbed. Fig. 1 is a photograph of this 100 mm CCR and one of the Apollo 11 CCR spares.

Fig. 1. Shows the Flight Certified 100 mm CCR that has been fabricated to the specifications with Apollo CCR. The offset angles for the back faces significantly exceeded the specifications, for two of the angle by almost a factor of two.

6. Thermal/optical performance challenges

One of the most critical challenges is the issue of heat flows or thermal gradients inside the CCR. Since the index of refraction of the fused silica depends upon temperature, thermal gradients in the CCR will cause the index of refraction to vary within the CCR and thus it will not act as a diffraction limited mirror. For this reason, we need to understand in detail the magnitude of the gradients caused by the various effects, then adjust the design to control these gradients and finally evaluate the performance with the control procedures in place. We first need to determine the heat deposition. This is accomplished using dedicated programs developed in parallel at Frascati and at the University of Maryland. To perform these simulations, we use Thermal Desktop, a software package of C&R Technologies of Boulder CO. This analysis yields a three dimensional matrix describing the temperature distribution in the CCR for a given configuration and set of parameters. These simulations are being carried out at Frascati and at the University of Maryland. A program developed at the University of Maryland using IDL of RSI Inc. converts the three dimensional temperature matrixes into a two dimensional phase front which captures the error induced by the temperature gradients. Both Code V and another IDL program developed at the University of Maryland are being used to convert the phase error into a far field diffraction pattern (FFDP) which defines the

strength of the signal that will be seen as a laser return at the ground station.

We now address the three primary sources of heat that cause the thermal gradients:

6.1. Absorption of solar radiation within the CCR

During the lunar day, the solar radiation enters the CCR and portions of this energy are absorbed by the fused silica. Since the different wavelengths in the solar radiation are absorbed with different "strengths" the heat is deposited in different proportions in different parts of the CCR. To address this, we must analyze each narrow spectral band (1 nm) of the solar radiation separately and then sum over the wavelength bands to determine the heat deposition at each node. Thus for each narrow band, we must determine the amount of energy in the AMOS2 solar spectrum [14]. We then use the band-by-band absorption data from Heraeus [13] to determine the "decay depth" in the fused silica. The dependence of the decay depth on wavelength is illustrated in Fig. 2. Using Beer's law and the solar spectrum, we may determine the amount of heat deposited at each node that a given ray passes through. This three dimensional matrix of heat inputs is then used as an input file to the Thermal Desktop in order to compute the thermal gradients.

6.2. Heat flux in mechanical mounting tabs

If the CCR is at a temperature that is different than the housing temperature there will be a flow of heat passing into (or out of) the housing to the tab of the CCR and then into the CCR. This in turn will cause a flow of heat within the CCR which produces irregularities in the temperature and then in the indices of refraction of the fused silica. This causes a degradation of the retroreflected beam and a reduction of the return signal to the ground station. For the Apollo arrays (and for the following satellite systems like LAGEOS) KEL-F rings that have a low conductivity have been used. However, this conductivity is unacceptably large for the LLRRA-21. In order to meet the requirements of the LLRRA-21, we have designed a modification of the KEL-F design that greatly reduces the conductivity but will also survive launch. This consists of 1 mm "pins" that provide a line contact, rather than the two dimensional contact of existing CCR mountings. The launch aspects of this design are considered in Section 12.

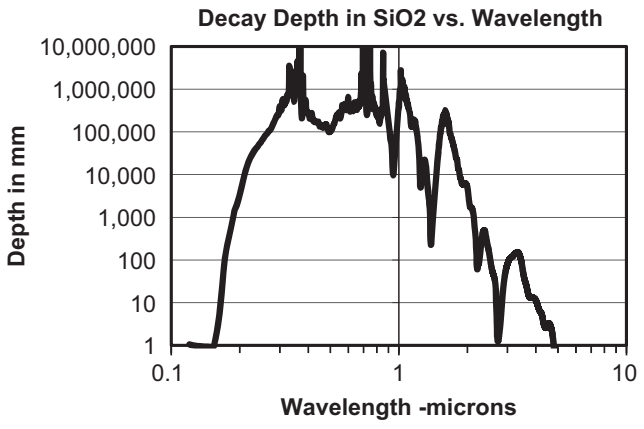

Fig. 2. Illustrates the exponential decay depth, used to determine where the solar radiation is deposited.

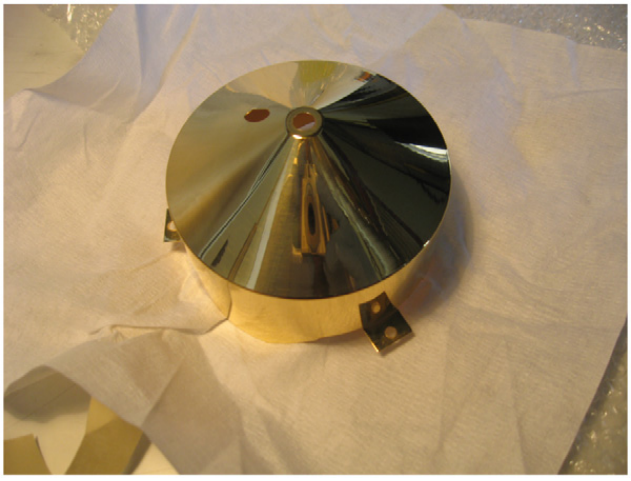

Fig. 3. Inner thermal shield with low emissivity (2%) gold coating on both the inner and outer surfaces made of LaserGold from Epner Technologies.

6.3. Radiation between CCR and surrounding pocket

In the case of the Apollo CCR arrays, the back surfaces of the CCR view the aluminum surface of the pocket in the housing. This is machined aluminum that has a relatively high emissivity/absorptivity. If the temperatures of the CCR and the aluminum are different there is a radiation exchange of thermal energy which in turn causes a flux in the CCR as the heat exits out of the front face to cold space. In the case of the Apollo arrays this has not been a serious issue, either in the analysis or in the performance of the arrays.

However, for the much larger LLRRA-21 it is more serious and we need to reduce this effect in order to maintain an acceptable tip-to-face temperature difference. Thus in order to combat this effect, we enclose the CCR in thermal shields that prevent this radiative flow of heat. This is accomplished by the use of two shields with a very low emissivity, (i.e., 2%) and that can be expected to maintain this low emissivity over a period of long time. Such a shield has been fabricated by Epner Technologies of Brooklyn, NY, in order to evaluate manufacturability and in order to perform the initial thermal/optical/vacuum tests to evaluate the effectiveness of this solution. Fig. 3 is a photograph of the inner thermal shield that was used in the April 2010 thermal/optical/vacuum tests.

7. Results of thermal simulation

In order to discuss the results of the thermal simulations in a form that addresses the required optical properties, we wish to determine the variation of the temperatures or the gradient from the Tip of the back of the CCR to the Front Face (TtFF). This directly affects the

divergence of the outgoing beam and thus the signal strength back on the earth. Thus we need to determine how this TtFF gradient changes during a lunation (i.e., the changing sun angle during the day/night cycle on the moon). For various sun angles, one obtains different magnitudes and distributions of the temperatures, as illustrated in Fig. 4. It is this gradient that will change the index of refraction and thus disturb the strength of the return beam to the earth. Fig. 5 is a plot of the variation of the gradient, through a full lunation, which is below 0.5 K for all but one or two days of the month. For most of the lunation, the worst of the performance is indicated in Fig. 6. For one or two days the performance is worse. Although this would be an acceptable situation, we believe that by modifying the sun shield and with a better selection of the shape and metal surfaces of the inner thermal shield, this can be brought below 0.7 K. We are still proceeding to optimize this design further. In addition, there are optical design procedures for the CCR that allow us to further reduce the effective temperature difference from the tip to the face. As a result, we have demonstrated (in computer simulation) that the thermal effects of the solar absorption, the mount conduction and the radiative exchange with the pocket can be controlled to a sufficient degree. Using Code V, we may simulate the

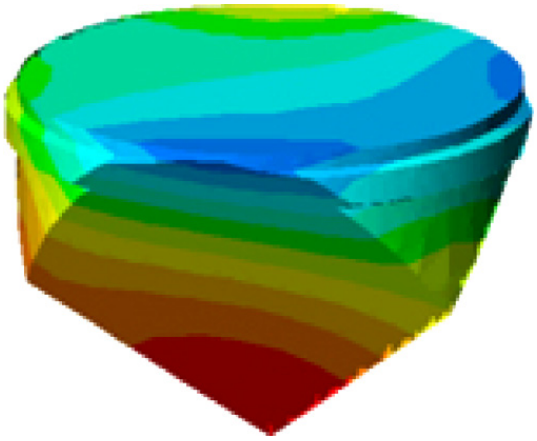

Fig. 4. A typical distribution of temperature in the CCR for a given set of conditions. This image is one in a series of day by day temperature distributions through a lunation. The temperatures illustrated by the colors range from 185.7 to 186.8 K.

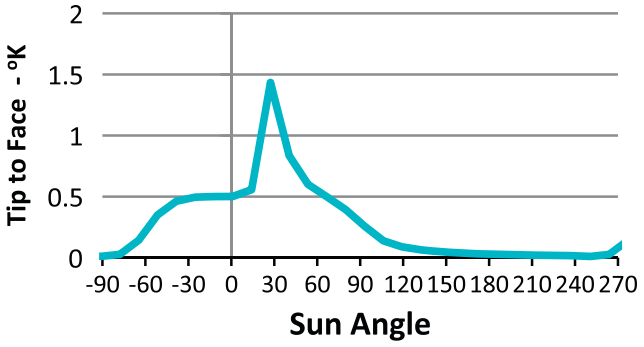

Fig. 5. Tip-to-face temperature variation over a single lunation. The peak represents breakthrough that would occur with the design of the sun shield shown in Fig. 11.

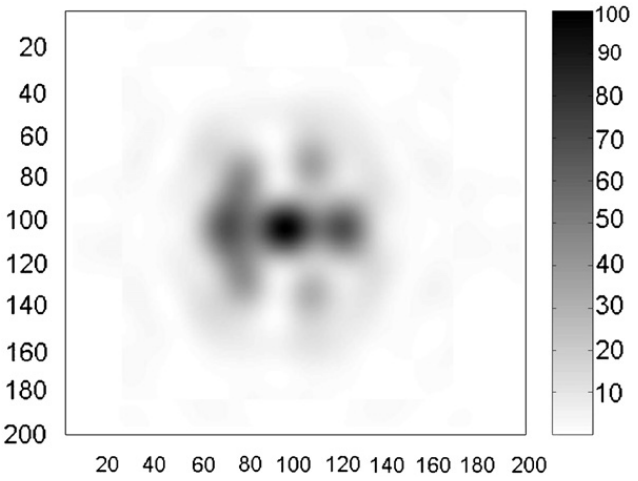

Fig. 6. This is the computer simulation for the far field diffraction pattern or beam distribution for a 100 mm CCR with a temperature gradient of 0.5 K. This has the measured offset angles of the CCR that was fabricated and shown in Fig. 1.

FFDP that is expected for a given axial thermal gradient. Thus the pattern for a CCR with the measured back surface offset angles and a thermal gradient of 0.5 K (the worst gradient in the computer simulation of all the thermal effects except for one or two days) is shown in Fig. 6. With the modified design, the signal return for various ground station latitudes and the expected selenographic coordinates will be computed for the full lunation cycle. This will be done with a sequence of programs, now being tested, which consist of a custom IDL program, Thermal Desktop by C&R Technologies program, Code V by OA Associates, and finally another custom IDL program.

8. Signal strength

In this section, we will address the role of the various effects on signal strength. This will be performed by comparison to the signal strength of the theoretical and actual return of the Apollo 15 array. The reason for selecting Apollo 15 as the reference is that this array is the most frequently observed, by both the APOLLO station at Apache Point [10] and the other lunar laser ranging stations.

8.1. Signal strength and on-axis return

The on-axis return (i.e., no velocity aberration) scales with the fourth power of the aperture diameter. Thus a single solid CCR of 100 mm will have a return that is greater than a single Apollo CCR of 38.1 mm by a factor of 47.5. Thus we have a return for a single 100 mm CCR that is 16% of the return of the entire Apollo 15 array consisting of 300 38.1 mm CCRs.

8.2. Signal strength and velocity aberration

The effect of velocity aberration (or the relative transverse velocity of the CCR w.r.t. the ground station) means that the return beam will be displaced from the

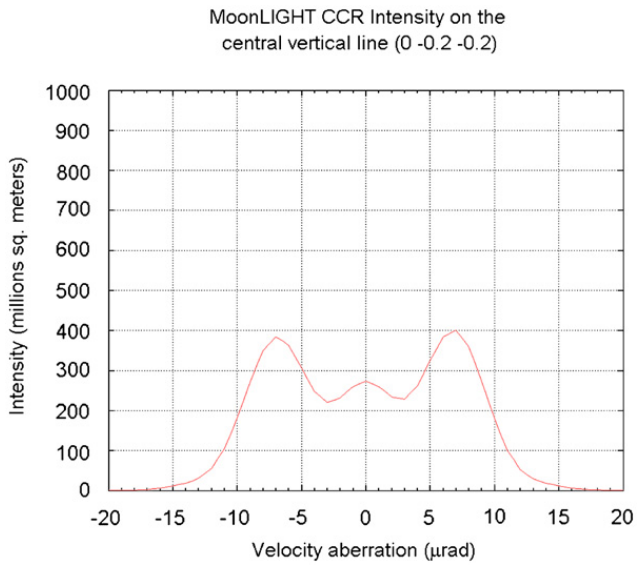

Fig. 7. This a computer simulation of an east-west cut for the far field diffraction pattern of a 100 mm CCR with two of the back surfaces having angular offsets of 0.2 arcsec.

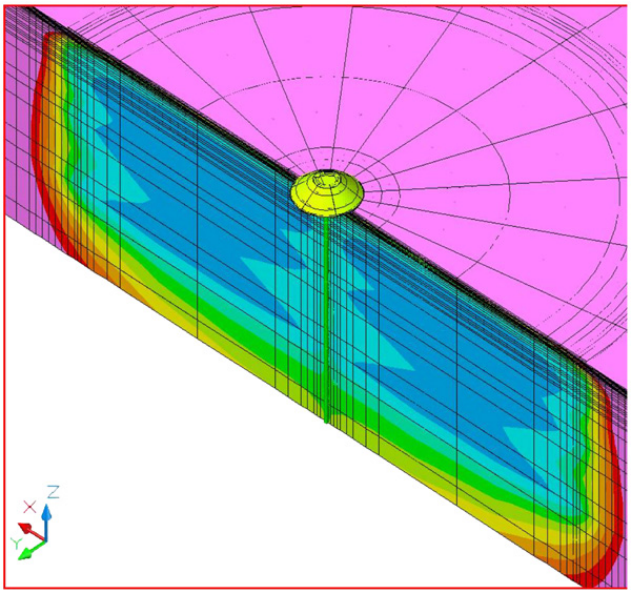

Fig. 8. Temperature distribution in the regolith with mushroom housing and 2 meter thermal blanket after equilibrium. The colors indicate the range of temperatures, from 70 to 170 K.

originating telescope in proportion to the relative linear velocity of the CCR and the ground station on earth. In order to recover most of the resultant loss of signal, we will offset the back angles of the CCR. This is the same procedure that is done for satellite retroreflector arrays, for which the velocity aberration is much greater than for the moon. However, since the relative motion of the array with respect to the ground station is always essentially in the East–West direction, we can do a much better job of mitigating the detrimental effects of velocity aberration as compared to the case of an earth orbiting satellite. By offsetting two of the back angles by 0.2 arcsec from their nominal value of 90°, the Cove V simulation produces the plot indicated in Fig. 7. The magnitude of the improvement depends upon the latitude of the ground station. Thus for a station latitude of 45°, offsetting the angles increases the signal by 55%. In this case, the signal is 60% of the on-axis return of the Apollo 11 array, or taking into account the dust degradation of the Apollo 11 array (see the section on "Signal Strength and the Dust Issue" below), the return will provide an improvement with respect to the current Apollo 11 signal strength of about 600%.

8.3. Signal strength and the thermal gradient

We address the dependence of the signal strength on the thermal gradient, a two step procedure. First the curvature of the wave front due to the axial thermal gradient is computed. This relates the curvature (or peak to peak value) of the curvature to the TtFF temperature difference. Then the on-axis degradation is computed using the wave front curvature with Code V. The result is shown in Fig. 6. This is combined with the reduction in the central intensity due to the TIR. This is somewhat conservative since it does not take into account the surrounding lobes from the TIR. The axial gradient is different for the surface emplacement (Fig. 7) and for the anchored emplacement (Fig. 8). It also varies throughout the lunar cycle. However, at this point, we have taken a typical value of 0.5 K. In this case, the result of the thermal degradation is to reduce the signal by about 20%. Thus the return of a single 100 mm CCR is about 4.8% of the theoretical Apollo 15 array of 300 CCRs. However, taking into account the dust issue (see next session) the return will be about half of the current operational return of the Apollo 15 array.

8.4. Signal strength and the dust issue

Recent analysis of the returns obtained by the Apollo station indicate that the rate of single photoelectron return is about a factor of ten less than the expected return rate [15]. While the reason for this is still under investigation the two main candidates are dust raised by the rockets used for the launch of the Lunar Excursion Module as the astronauts left the surface of the moon, or the accumulation of levitated dust on the front surface of the CCR over the decades. Concerning a robotic mission (which will be the first set of missions), the dust will be raised on landing. Our current design will have a "dust cover" in place during landing. Therefore this problem will not arise (since the Lander will obviously not take off as did the LEM).

Concerning the accumulation of the dust, the sunshade will significantly reduce in the quantity of dust that reaches the surface of the CCR. In addition, we are investigating a "dust filter" that may further reduce the dust reaching the CCR. In any case, this should not be a significant problem during the first decade of operation. Thus we may expect over the first decade an increase in the signal by about a

factor of ten. Thus, the single 100 mm CCR will have about 48% of the rate of return of the 300 CCRs in the Apollo 15 array in its current condition.

8.5. Signal strength, libration and range accuracy

However, the above discussion has neglected the primary reason for proposing a large single CCR (or an array of five spatially separated large single CCRs). The lunar librations cause the Apollo 15 array to tilt by up to $\sim 10^{\circ}$. Thus even if we transmitted an extremely narrow laser pulse, it would return spread in time since some would be reflected from a near CCR and some would be reflected from a far CCR. The magnitude of this effect depends upon the dimensions of the Apollo retroreflector array and the libration angles of the moon. For Apollo 15 at the extreme libration angles, the FWHM of the return pulse may be 1 ns or result in an r.m.s. of ~ 75 mm in range. On a good night, the APOLLO station then collects ~ 6000 photoelectrons to obtain a range accuracy of ~ 1 mm. Since the APOLLO station has a 3.5 m telescope, the collection of this many return photoelectrons can be accomplished. However, the purpose of the large single CCR is that there is no spreading due to the librations. Thus, in principle, one needs to collect only a single photoelectron to obtain the same 1 mm r.m.s. Obviously one needs a few more, since it is the agreement in the range of several successive photoelectrons that assures a lunar detection. When the first author was Scientific Director of the initial lunar laser ranging station at McDonald Observatory, ranging would stop after the reception of four or five photoelectrons. Thus comparing the APOLLO 3.5 m telescope to 1.00/0.75/0.50 m telescopes, the 6000 returns in 10 min at the APOLLO station is equivalent to 235/132/55 returns, by far enough for accurate ranging. Of course, obtaining 1 mm accuracy with a single shot during an entire lunation implies that the current ground stations are upgraded to have a laser shorter than 7 ps, a detector and timing electronics that have an accuracy of ~ 7 ps and good offset pointing.

9. Thermal challenges

9.1. Overall with housing and regolith

In the analysis of the previous section, in order to address a surface emplacement, we have assumed certain parameters for the regolith and other effects, etc. However, we now address an anchored emplacement, in which one must develop an integrated model which contains a housing design, a model for the behavior of the regolith and the coupling of these effects. Such a model has been developed and the thermal behavior simulated through a full lunation. This has been parameterized to agree with the heat flow experiment deployed during the Apollo 16 mission. The results of one such run are shown in Fig. 8, in which one has included the effect of the support rod (discussed in the next section), the solar effect on the housing, the thermal blanket and so on. The solar blanket isolates the regolith from the direct thermal input of the sun. In turn, this shields the support rod from the temperature extremes it would encounter in the unshielded regolith. See Fig. 8 for the effects under and beyond the blanket. Various runs have been made to evaluate the advantages. In particular, this uses the earlier "mushroom" (i.e., descriptive of the shape of the design) design of the housing and uses an aluminum support rod. The circular region surrounding the housing is a thermal blanket to reduce the temperature variations surrounding the support rod. In fact, the plot of the temperature gradient across the CCR shown in Fig. 4 was derived by this "whole" model. Again, Fig. 8 is one frame in a sequence that covers an entire lunation. The evaluation of a single lunation is performed after evaluating many successive lunations (~ 1000) in order to reach the "final state" distribution.

10. Emplacement challenge

To attain the required mechanical stability w.r.t. the center of mass of the moon, we must address the temperature distribution in the regolith, the effects of the thermal blanket and the effects of heat conduction in the support rod. A locking depth is chosen to reduce thermal motion. The blanket further reduces the thermal effects and the effects on the support rod. This simulation cycles through the lunation and annual cycles.

11. Current housing designs

We are successively refining our design based upon maximizing the overall performance by jointly optimizing the behavior with respect to the various are successively refining our designs based upon optimizing the behavior with respect to the various different phenomena that affect the overall performance. This has been addressed

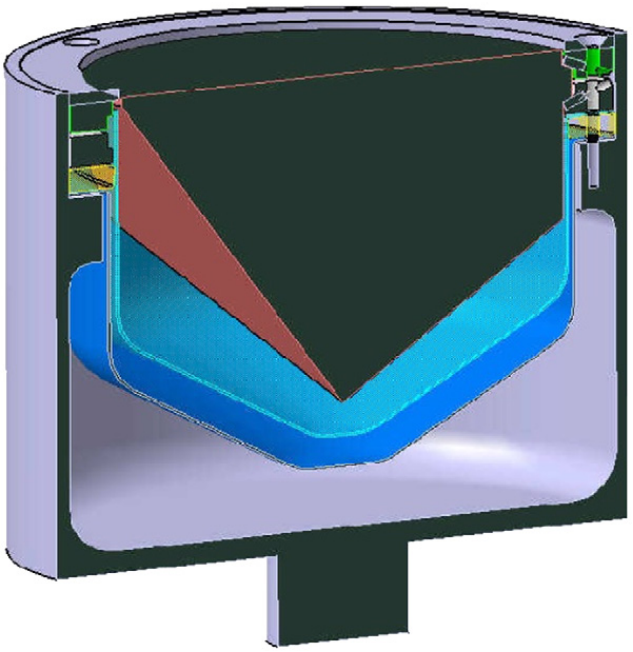

Fig. 9. This illustrates more detail within the current design housing.

using the computer simulations discussed in the above sections and using the data obtained with the thermal vacuum with the thermal vacuum measurements. This addressed both the design for the manned emplacement and the use of the 100 mm solid CCR package on various robotic missions such as the ILN, Lunette and possible X-Google missions. Fig. 9 illustrates the current design for the housing. In Fig. 10, an exploded version illustrates in more detail the individual components and how they interact. Fig. 11 is the configuration that was used for the above simulations. Figs. 9 and 10 also illustrates the design that is most similar to the configuration that is being used in the April 2010 thermal/optical/vacuum tests. Fig. 11 is a photograph of the package that was used in the April 2010 tests. It has the sun shade which is not indicated in Figs. 9 and 10. Other designs have been addressed for the Italian Space Agency MAGIA mission [16,17], lunar orbiter mission for gravity and gravitational red-shift measurements which will carry our 100 mm CCR into lunar orbit (if and when it receives final approval).

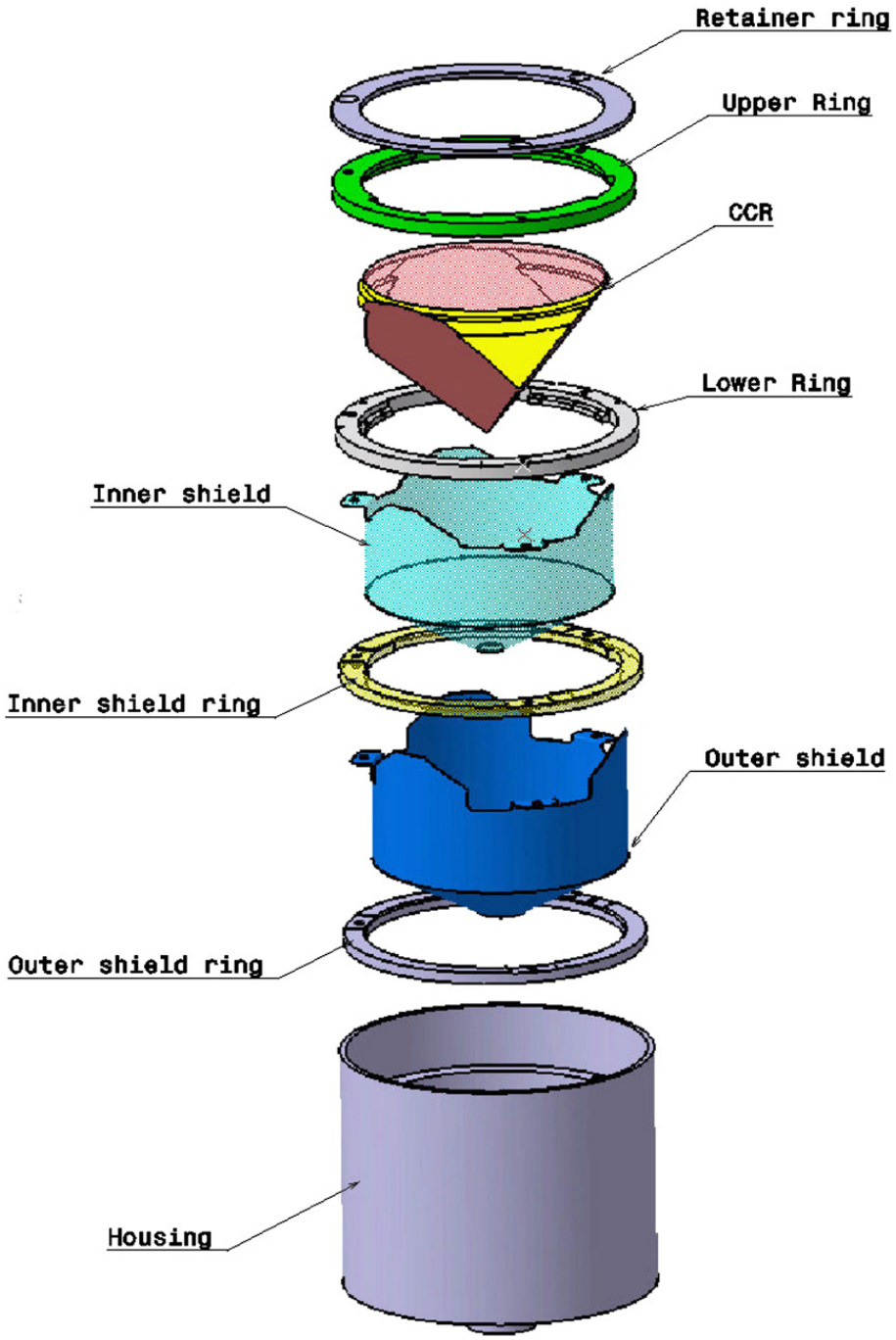

Fig. 10. This is an exploded view of the current status of the design. It is this design, with the addition of the sun shade that has been used in the most recent thermal-optical-vacuum tests in Frascati, Italy.

Fig. 11. This is a hardware implementation of the current LLRRA-21 package design. This unit, with the sun shade, was tested in the thermal/optical/vacuum system in Frascati in April 2010.

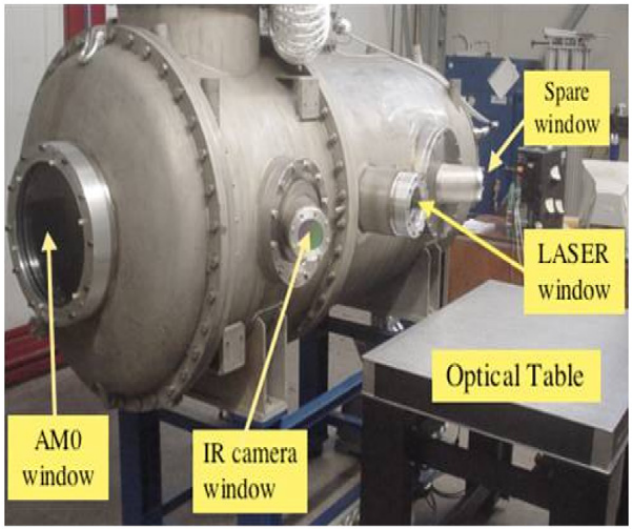

Fig. 12. SCF (thermal/optical/vacuum chamber in Frascati) indicating the windows for various functions.

12. Thermal vacuum chamber testing

Up to this point, the discussions have addressed concepts for the LLRR-21 and thermal and optical computer simulation developed to validate the design concepts. We now address the thermal/optical/vacuum testing to further validate the design issues. To accomplish this, we need to provide two classes of measurements in the SCF shown in Fig. 12. The first is the thermal

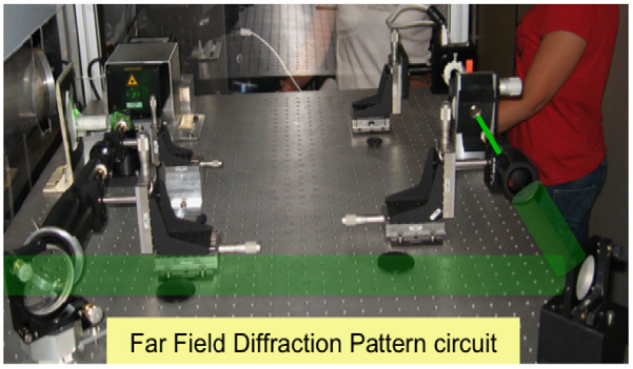

Fig. 13. Optical table for measuring the far field diffraction pattern of the CCR while the latter is in vacuum and being illuminated by the solar simulator.

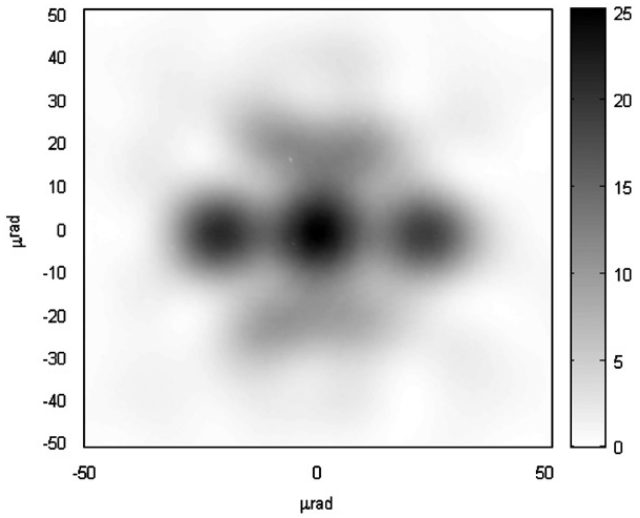

Fig. 14. This is a sample of the FFDPs obtained during the April 2010 thermal/optical/vacuum tests. This is a very preliminary test.

behavior of the test configuration. A solar simulator that has a good representation of the AMO2 solar spectrum is used to provide the solar input. To evaluate the thermal performance of the designs, we use both thermo-resistors and an infrared video camera. The former must be specially configured in order that the wires not conduct more heat than the test item. The latter yields temperatures over the entire test object at each instant. On the other hand, to address the relation between the thermal performance and the optical performance, we currently use the optical configuration shown in Fig. 13 to measure the far field diffraction pattern shown in Fig. 14. This is the crucial test of a CCR package and is performed with the CCR in the chamber. However, the measurements during the April 2010 tests must be regarded as preliminary w.r.t. the full simulation. The inner thermal shield that is defined by our current design was not available in time for the test. The optical configuration for determining the far field diffraction pattern did not fully illuminate the full 100 mm aperture of the CCR. For the next run, we plan to implement a phase front measurement. While the far field diffraction pattern measures the ultimate specification for the system, it is not as effective

in detecting the source of a problem as is the data from a wave front measurement. Various configurations and designs of the CCR and the housing have been and are being tested in the SCF Facility at INFN-LNF in Frascati, Italy with the solar simulator, the temperature data recording with an infrared camera and the measurement of the far field diffraction pattern (FFDP).

13. Launch requirements

We are just beginning a study of the requirements of launch. This particularly addresses issues of the support of the CCR by the tabs in the vibration and acceleration environment of the launch. To this end, we have formulated a first example of a structural analysis with the ANSYS program addressing both the tab/ring configuration and the resonant effects on the inner and outer thermal shields [18,19]. While the Apollo CCRs were supported by the tabs in contact with the KEL-F rings, this configuration has too high a thermal conductivity for the LLRRA-21. Therefore we are employing a "line contact" to reduce the conductivity. This line contact consists of a cylindrical "pin" upon which the tab rests. However, this is more vulnerable to the stress of launch. Thus we are addressing the contact between the CCR edge (i.e., the three tabs on the side of the CCR) and KEL-F pins in the support plastic rings made of KEL-F. This analysis addresses the stability and strength of the tab support and the KEL-F line support for 10 g launch accelerations (e.g., an evaluation in excess of the 6 Gs characteristic of the ATLAS V launch specifications). The model used to perform this analysis is indicated in Fig. 15. The sloping cylindrical section is the "pin" that is used for the low conductance support. At the left is the tab of the CCR. The first issue stresses the stress level, that is, will this exceed the elastic limit of the KEL-F. That is, is the stress sufficiently great to exceed the yield strength of the pin, to cause a permanent deformation? Fig. 16 indicates the stress levels. The maximum stress level is somewhat below the elastic limit. However, we will bevel or round the edge of the table to greatly improve the situation. An ANSYS analysis of this is in progress. The second issue is the magnitude of the deformation of the pin under the stress, which is addressed in Fig. 17. The deformation is indicated in Fig. 17. We are also performing a modal structural analysis of the inner gold plated thermal shield for an ATLAS V launch. A new analysis is addressing the advantage of rounding the edge of the tab and reducing the diameter of the rod or changing the material of the rod. This will allow the tab to rest on the KEL_F ring instead of the rod, thus providing much greater support. This would appear to provide a factor of ten or more improvement.

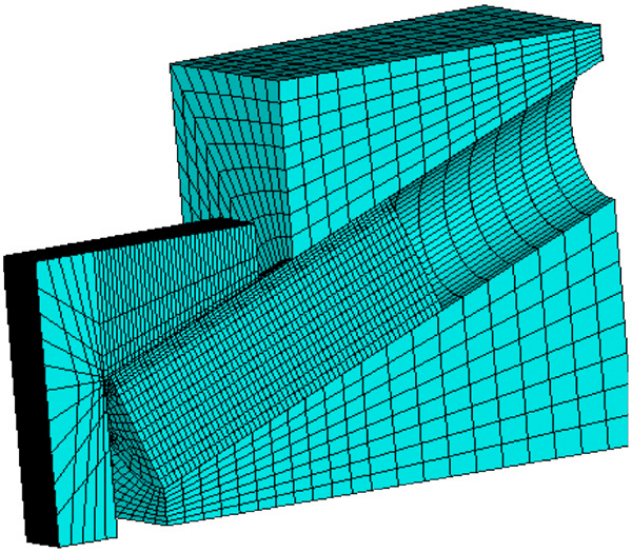

Fig. 15. ANSYS model for CCR tabs and the KEL-F ring and pin support.

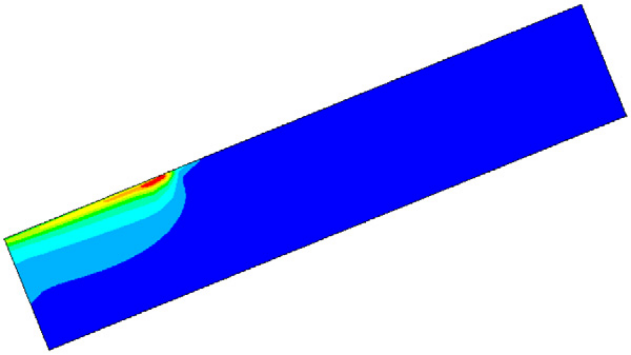

Fig. 16. Stresses in the pin for a 10 g load. The maximum stress is 27 Mpa as compared to yield strength of 32 Mpa.

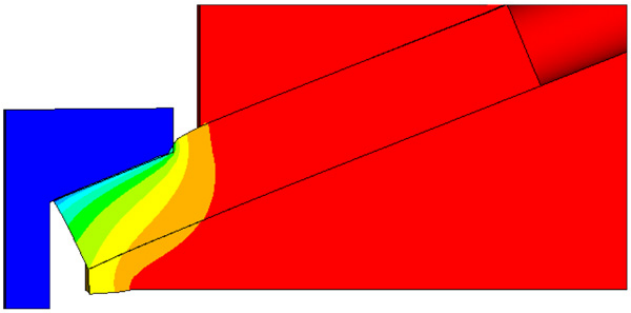

Fig. 17. Deformation in the Pin and Ring under the 10 g load. The maximum deformation is 9.7 microns.

14. Emplacement

In order that the CCR be isolated from the diurnal thermal effects from lunar day to lunar night (the regolith will rise and fall by 200–400 μm), we need to escape the effects of the diurnal temperature changes. To do this, we plan to drill down to a depth of ~1 m, where the changes in temperature are essentially negligible and anchor a support rod at this depth. While this can be accomplished for a manned mission in the manner used in Apollo for the heat flow experiment the emplacement on a robotic mission such an ILN requires a new approach.

One very interesting approach, pneumatic drilling, has been developed by HoneyBee, Inc. (New York, New York). In this approach the debris developed in the drilling

operation is removed from the hole by a jet of gas at the tip of the drill. This causes the debris to flow up to the surface and out of the hole as illustrated in Fig. 18. Thus it is not necessary to compress the regolith, which is the reason that some other drilling procedures need large forces. The pneumatic drilling has been extensively tested in stimulants of the lunar soil, in vacuum and in both earth and lunar gravity. Due to its relative availability on the Lander, we will consider the use of existing helium as the carrier gas rather than the nitrogen that has been used in the tests to date. HoneyBee is also developing approaches to mounting the pneumatic drill on a rover in the manner of what would be required for the ILN. One approach to this is indicated in Fig. 19.

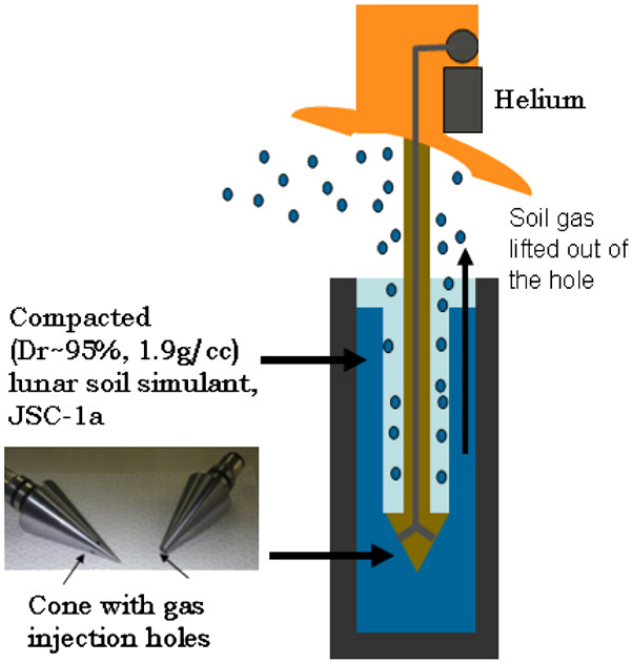

Fig. 18. Illustration of the gas convected drilling or pneumatic drilling developed by Honeybee.

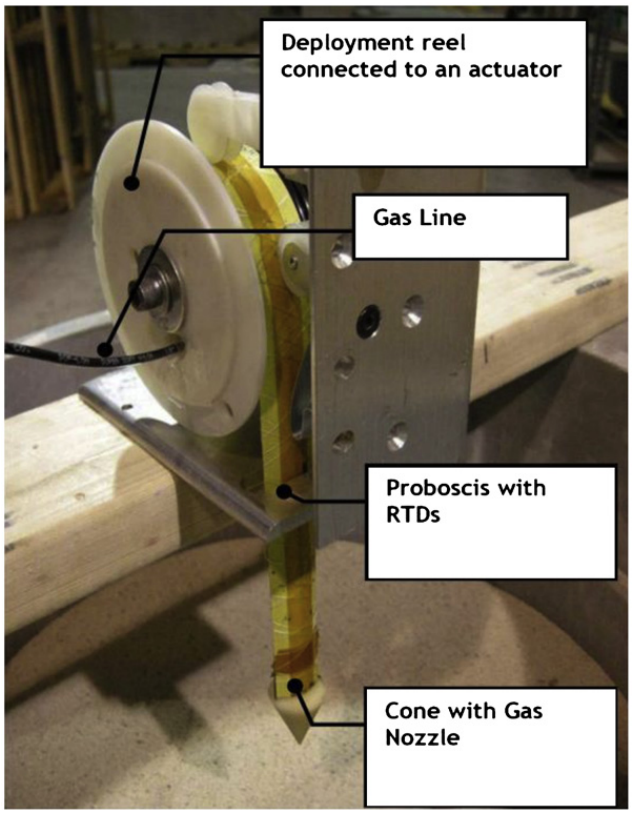

Fig. 19. Example of an implementation of robotic drilling for lunar emplacement.

15. Challenges and objectives

In this section, we address the challenges that are still present in order to assure the feasibility of the experiment, the proper operation of the package on the surface of the moon and the withstanding of the launch conditions:

(1) Continue simulations to optimize thermal performance, i.e. minimize the TtFF gradient
   a. Evaluate further modifications of the housing structure and the support rod.
   b. Investigate optical procedures to minimize the beam spreading for a TtFF gradient.
   c. Optimize the offset of the back faces to minimize the impact of velocity aberration.
(2) Continue further thermal vacuum testing of designs at SCF in Frascati
   a. Evaluate different design options
      i. NASA Manned Lunar Landing
      ii. MAGIA—The Italian Space Agency Lunar Orbiter
      iii. ILN—The International Lunar Network Anchor Nodes
   b. Validate thermal modeling and simulations
(3) Investigate new lunar regolith drilling capabilities
   a. Investigate Honeybee gas assisted drilling
   b. Investigate robotic capabilities for ILN missions
   c. Investigate strategies for robotic emplacement of CCR
   d. Collaboration on drilling technologies with heat flow experiments
   e. Field tests of new drilling techniques in a simulated lunar regolith
(4) Analyze various sun shading designs
(5) Analyze launch requirements

16. Mission opportunities

The initial approach of our LLRRA-21 program was to define a package that would allow a very significant improvement in the accuracy of lunar laser ranging in order to support the new vistas of lunar science, general relativity and cosmology. This initial effort was addressed to the next NASA Manned Lunar Landings and the research was supported by the Lunar Science Sortie Opportunities (LSSO) program out of NASA Headquarters.

However, since then several other opportunities have arisen. The International Lunar Network (ILN) has been

proposed by NASA, which consists of the launch of four "Anchor Nodes" in about 2015. This is a robotic mission. The initial specification of the payload will contain a 100 mm CCR for Lunar Laser Ranging.

Several other robotic missions are now under consideration. The Lunette mission would be an explorer mission for which the LLRRA-21 is a backup option. Lockheed Martin is considering an internally developed lander and there are several X-Google participants that are considering providing space on their vehicle. In addition, a Phase Study for the Italian Space Agency for the MAGIA mission [16,17], which is a lunar orbiter, has been completed. The MAGIA spacecraft would include our LLRRA-21. It is awaiting a down selection in preparation to funding for the flight approval. This effort is being supported by a recently approved MoonLIGHT program at INFN-LNF.

Teams of collaborators

LSSO team

Centered at the U. of Maryland, College Park

This was the initial group that addressed the LLRRA-21 concept with Professor Currie. The collaborative research effort was then supported by the Lunar Science Sortie Opportunities (LSSO) program at NASA headquarters. The members of this team are:

Douglas Currie PI	U of Maryland, College Park, College Pk, NLSI, Moffett Field, CA & INFN-LNF Frascati, Italy
Bradford Behr	University of Maryland, College Park, MD
Tom Murphy	University of California at San Diego, San Diego, CA
Simone Dell'Agnello	INFN/LNF Frascati, Italy
Giovanni Delle Monache	INFN/LNF Frascati, Italy
W. David Carrier	Lunar Geotechnical Institute, Lakeland, FL
Roberto Vittori	Italian Air Force, ESA Astronaut Corps
Ken Nordtvedt	Northwest Analysis, Bozeman, MT
Gia Dvali	New York University, New York, NY and CERN, Geneva, CH
David Rubincam	GSFC/NASA, Greenbelt, MD
Arsen Hajian	University of Waterloo, ON, Canada

MoonLIGHT team

Centered at the INFN-LNF in Fracati, Italy

This group at the Istituto Nazionale di Fisica Nucleare - Laboratori Nazionali di Frascati (INFN-LNF) in Frascati, Italy has developed the SCF (i.e., the thermal vacuum chamber) and collaborated in developing models and simulations supporting the LLRRA-21 program. This group has been supported by internal INFN funds:

Simone Dell'Agnello PI	INFN-LNF, Frascati, Italy
Giovanni Delle Monache	INFN-LNF, Frascati, Italy
Douglas Currie	U. of Maryland, College Park, MD, NLSI, Moffett Field, CA & INFN-LNF
Roberto Vittori	Italian Air Force & ESA Astronaut Corps
Claudio Cantone	INFN-LNF, Frascati, Italy
Marco Garattini	INFN-LNF, Frascati, Italy
Alessandro Boni	INFN-LNF, Frascati, Italy
Manuele Martini	INFN-LNF, Frascati, Italy
Nicola Intaglietta	INFN-LNF, Frascati, Italy
Caterina Lops	INFN-LNF, Frascati, Italy
Riccardo March	CNR-IAC & INFN-LNF, Rome, Italy
Roberto Tauraso	U. of Rome Tor Vergata & INFN-LNF, Frascati
Giovanni Bellettini	U. of Rome Tor Vergata & INFN-LNF, Frascati
Mauro Maiello	INFN-LNF, Frascati, Italy
Simone Berardi	INFN-LNF, Frascati, Italy
Luca Porcelli	INFN-LNF, Frascati, Italy
Giuseppe Bianco	ASI Centro di Geodesia Spaziale (CGS) "G. Colombo", Matera

Acknowledgements

We wish to acknowledge the support of the University of Maryland via the NASA "Lunar Science Sortie Opportunities" (LSSO) program (Contract NNX07AV62G) to investigate Lunar Science for the NASA Manned Lunar Surface Science and the LUNAR consortium (http://lunar.colorado.edu), headquartered at the University of Colorado, which is funded by the NASA Lunar Science Institute (via Cooperative Agreement NNA09DB30A) to investigate concepts for astrophysical observatories on the Moon. In support of the research at Frascati, we wish to acknowledge the support of the Italian Istituto Nazionale di Fisica Nucleare, Laboratori Nazionali di Frascati (INFN-LNF). We also wish to thank the Italian Space Agency (ASI) for the support during the 2007 lunar studies and the 2008 Phase A study for the proposed MAGIA mission. The first author would also like to acknowledge helpful conversation with Jack Schmidt, Ken Nordtvedt and Ed Aaron.

References

[1] P.L. Bender, D.G. Currie, R.H. Dicke, D.H. Eckhardt, J.E. Faller, W.M. Kaula, J.D. Mulholland, H.H. Plotkin, S.K. Poultney, E.C. Silverberg, D.T. Wilkinson, J.G. Williams, C.O. Alley, The Lunar Laser Ranging Experiment, Science 182 (4109) (1973) 229–238.

[2] D.G. Currie, S. Dell'Agnello, G. Delle Monache, T. Murphy, R. Vittori, D. Carrier, C. Cantone, M. Garattini, A. Boni, M. Martini, C. Lops, N. Intaglietta, G. Bellettini, R. Tauraso, R. March, G. Bianco, D., Rubincam, A Lunar Laser Ranging Retro-Reflector Array for NASA's Manned Landings, in: the International Lunar Network and the Proposed ASI Lunar Mission MAGIA Sixteenth International Workshop on Laser Ranging Instrumentation Poznan Poland, 13–17 October 2008, pp. 277–283.

[3] J.T. Ratcliff, J.G. Williams, S.G. Turyshev, Lunar science from laser ranging—present and future, in: 39th Lunar and Planetary Science Conference, (Lunar and Planetary Science XXXIX), held March 10–14, 2008 in League City, Texas. LPI Contribution No. 139, p.1849.

[4] The MAGIA prime contractor is Rheinmetall talia SpA; the MAGIA PI is Angioletta Coradini of INAF-IFSI.

[5] J.G. Williams, D.H. Boggs, J.T., Ratcliff, A larger lunar core? in: Proceedings of the 40th Lunar and Planetary Science Conference, (Lunar and Planetary Science XL), held 23–27 March 2009 in The Woodlands, Texas, id.1452.

[6] J.G. Williams, S.G. Turyshev, Dale H. Boggs, Lunar laser ranging tests of the equivalence principle with the Earth and Moon, International Journal of Modern Physics D 18 (2009) 1129–1175.

[7] N. Rambaux, J.G. Williams, D.H. Boggs, A dynamically active moon—lunar free librations and excitation mechanisms, in: Proceedings of the 39th Lunar and Planetary Science Conference, (Lunar and Planetary Science XXXIX), held 10–14 March 2008 in League City, Texas. LPI Contribution No. 1391, Abstract # 1769.

[8] J.G. Williams, D.H. Boggs, J.T. Ratcliff, Lunar tides, fluid core and core/mantle boundary, in: Proceedings of the 39th Lunar and Planetary Science Conference, (Lunar and Planetary Science XXXIX), held 10–14 March 2008 in League City, Texas. LPI Contribution No. 1391, Abstract # 1484.
[9] K. Nordtvedt, Lunar laser ranging: a comprehensive probe of post-Newtonian gravity Gravitation: From the Hubble Length to the Planck Length, in: Ignazio Ciufolini, Eugenio Coccia, Vittorio Gorini, Roberto Peron (Eds.), Nicola Vittorio, Institute of Physics Publishing, the Institute of Physics, London, 2005, p. 97 Published by.
[10] T.W.Murphy,E.G. Adelberger,J.D. Stras-burg, C.W. Stubbs, K. Nordtvedt, Testing gravity via next-generation lunar laser-ranging, Nuclear Physics B Proceedings Supplements, vol. 134, pp. 155–162.
[11] K. Nordtvedt, Testing the equivalence principle with laser ranging to the Moon, Advances in Space Research, 32, 7, pp. 1311–1320.
[12] Dvali, G.; Gruzinov, A.; and Zaldarriaga, M. The accelerated Universe and the Moon Physical Review D, 68, 2, id. 024012.
[13] 〈http://optics.heraeus-quarzglas.com/en/ products applications/ productdetail_4105.aspx〉.
[14] ASTM E40090 Solar Constant and Zero Air Mass Solar Spectral Irradiance.
[15] T. Murphy, Long-term degradation of optical devices on the moon, Icarus 208 (2010) 31–35.
[16] S. Dell'Agnello, D. Currie, G. Delle Monache, R. Vittori, G. Bellettini, R. March, R. Tauraso, A. Boni; C. Cantone, M. Garattini, C. Lops, M. Martini, C. Prosperi, Fundamental Physics with the ASI Lunar Mission MAGIA (Phase A Study) NLSI, in: Proceedings of the Lunar Science Conference, held July 20–23, July 20–23, 2008 at NASA Ames Research Center, Moffett Field, California, LPI Contribution No. 1415, abstract no. 2146.
[17] ASI call document DC-PRZ-2007–002, Invitation to the Presentation of Proposal for Small Missions.
[18] F., Prete Contact Structural Analysis of the MoonLIGHT Laser Retro-reflector Assembly with ANSYS Bachelor Thesis (unpublished), Dipartimento di Meccanica e Aeronautica, University of Rome "Sapienza".
[19] A., Minghiglioni Modal Analysis of the MoonLIGHT Laser retro-reflector Assembly with ANSYS Bachelor Thesis (unpublished), Dipartimento di Meccanica e Aeronautica, University of Rome "Sapienza".